Article

New Catalysts Based on Silicon Carbide Support for Improvements in the Sulfur Recovery. New Silicon Carbide Nanotubes as Catalyst Support for the Trickle-bed H₂S Oxidation

Nicolas Keller, Ricardo Vieira*, Jean-Mario Nhut, Cuong Pham-Huu and Marc J. Ledoux

Laboratoire des Matériaux, Surface et Procédés pour la Catalyse, Université Louis Pasteur, UMR 7515 CNRS, 25 rue Becquerel, 67087 Strasbourg Cedex 2, France

Nanotubos de carbeto de silício (SiC) foram preparados a partir da reação gás-sólido entre vapor de SiO e nanotubos de carbono. A fase ativa NiS$_2$ suportada em nanotubos de SiC apresentou maior atividade catalítica e maior capacidade de armazenamento de enxofre na reação de oxidação seletiva do H$_2$S a enxofre elementar, em reator do tipo *trickle-bed*, que a mesma fase ativa suportada em grãos de SiC. O melhor desempenho deste catalisador foi explicado pela ocorrência do efeito de confinamento no interior dos nanotubos de SiC; ou seja, pelo aumento artificial da pressão parcial de H$_2$S no interior dos nanotubos em relação à mesma pressão fora dos nanotubos, resultando assim em um aumento na taxa da oxidação, uma vez que a velocidade de reação do H$_2$S é de primeira ordem. O catalisador suportado em nanotubos de SiC apresentou elevada resistência ao carregamento de enxofre devido a uma peculiar evacuação do enxofre pelo vapor de água condensado, permitindo assim uma limpeza contínua dos sítios ativos. A maior capacidade de armazenamento do enxofre sólido no suporte a base de nanotubos de SiC foi atribuído ao seu maior volume específico disponível para o armazenamento do enxofre do que o do suporte a base de grãos de SiC.

Silicon carbide nanotubes were prepared *via* a gas-solid reaction between SiO vapor and carbon nanotubes. The NiS$_2$ active phase on this support displayed both a high catalytic activity and high solid sulfur storage capacity in the trickle-bed selective oxidation of H$_2$S into elemental sulfur as compared to the grain-based SiC catalyst. The hypothesis of a confinement effect inside the SiC nanotubes has been put forward to explain the catalytic results. An artificial increase in the H$_2$S partial pressure inside the tubes when compared to the H$_2$S partial pressure outside the tubes would lead to an increase in the oxidation rate, due to the first order reaction rate toward H$_2$S. The SiC nanotube supported catalyst displayed very high resistance to the sulfur loading, due to a peculiar mode of sulfur evacuation by condensed steam which allows the continuous cleaning of the active site. The high solid sulfur storage capacity was due to a much larger void volume between each SiC nanotube available for the sulfur storage, than the void volume of SiC support with a grain size morphology.

Keywords: silicon carbide, nanotubes, H₂S oxidation, sulfur recovery, confinement effect

Introduction

The selective catalytic oxidation of H$_2$S by oxygen into elemental sulfur is the most interesting and efficient way for removing last traces of H$_2$S from waste acid gases generated by petrochemical refineries or natural gas plants.[1,2] This reaction is of high environmental interest, due to the high toxicity of H$_2$S. This reaction is also interesting from an economical point of view, leading to the transformation of a hazardous compound into a more valuable one for further chemical processes. The direct oxidation of H$_2$S into elemental sulfur has been developed,

in order to meet ever newer and stricter legislation requirements, that the well-known modified Claus process could not reach.[1] Industrial processes and recent developments have been reported in Part I of the present paper and summarized in a series of reviews published in the literature.[2,3] Previous works showed the very high performances obtained on silicon carbide grains or extrudates (SiC) supported catalysts as compared to the literature and industrial catalysts, especially at the low temperature of 60 °C.[4-7] The H$_2$S oxidation at low temperature is performed in a trickle-bed mode, the water of the inlet feed condensing at the head of the catalyst bed and trickling down through the catalyst. Such a trickle-bed mode, close to a liquid-phase mode, led to consider

that SiC nanotubes could be efficiently used as catalyst support compared to a macroscopic SiC support, by comparison with carbon nanotubes or nanofibers, which increase the catalytic efficiency when compared to carbon grains in liquid-phase applications.[8]

The aim of this article is to report the synthesis of SiC nanotubes via a gas-solid reaction.[9-13] and their use as catalyst support for the trickle-bed oxidation of H_2S into elemental sulfur at 60 °C.

Experimental

Catalyst preparation

Purified commercial multi-walled carbon nanotubes (MWNTs), supplied by Applied Science Ltd (Ohio, USA) were reacted with SiO vapor at 1200-1250 °C, leading to the formation of SiC nanotubes. MWNTs were directly used without any pretreatment. They had mean inner and outer diameters of *ca.* 30 nm and 100 nm, and lengths up to hundred micrometers. They showed a specific surface area of 20 m^2 g^{-1} with no microporosity. Residual metallic iron with a concentration of *ca.* 0.2 wt. %, previously used for the MWNTs synthesis, is encapsulated into the graphene layers, those particles thus being not accessible to the gas phase during any further treatments and reactions.

The SiC nanotubes obtained were calcined at 600 °C for 2 h in air to burn the remaining unreacted core carbon, as described by Keller *et al.*[9] The nickel-based catalyst was prepared by incipient wetness impregnation of the SiC nanotube support with an aqueous solution of $Ni(NO_3)_2.H_2O$ (Merck). It was dried at 120 °C for 14 h and then calcined at 350 °C for 2 h in order to decompose the nitrate salt and to form nickel oxide. The SiC nanotube supported NiS_2 catalyst was obtained by sulfidation of its corresponding oxide by reaction with a H_2S (4 vol. %)/He flow at 300 °C for 4 h (100 mL min^{-1} for 5 mL of catalyst corresponding to a catalyst weight of 3.35 g). The NiS_2 nature of the supported phase after sulfidation has been determined by XRD.[3] The loading of Ni was set at 5 wt. % and confirmed by the atomic absorption spectroscopy technique, performed at the Service Central d'Analyse of the CNRS (Vernaison, France). It should be noted that the residual iron, *i.e.*, *ca.* 0.2 wt. %, coming from the starting MWNTs, was not active for the H_2S oxidation under the experimental conditions used.

Micropilot description and characterization techniques

The description of the H_2S oxidation set-up has been reported in the companion paper.[3] The weight hourly space velocity (WHSV) was defined as the ratio of the inlet H_2S weight per hour to the weight of catalyst used.

Structural characterization of the samples was done by powder XRD measurements, carried out with a Siemens Diffractometer Model D-5000, using a Cu K_α radiation and operating at 40 kV and 20 mA. The nature of the crystalline phase in the sample was checked using the data base of the Joint Committee on Powder Diffraction Standards (JCPDS). Surface areas were measured by means of a commercial BET unit (Coulter Model SA 3100) using N_2 adsorption at –196 °C. The surface area was the surface calculated from the N_2 isotherm using the BET method. The micropore content was obtained from the *t*-plot method in conjunction with the Harkins-Jura thickness equation. Scanning Electron Microscopy (SEM) was performed on a JEOL JMS840 working at 20 mA with an accelerating voltage of 20 kV.

Results and Discussion

SiC nanotube synthesis

The XRD pattern of the SiC nanotubes only displayed diffraction lines corresponding to SiC crystallized in the low temperature β-face centered cubic structure, together with the low angle peak assigned to the non reacted remaining carbon (Figure 1). No traces of silica or silicon were detected, meaning that such species, if present, were only in an amorphous form, in very small amounts or very highly dispersed. After calcination at 600 °C for 2 h, the peak at low diffraction angles had disappeared and only
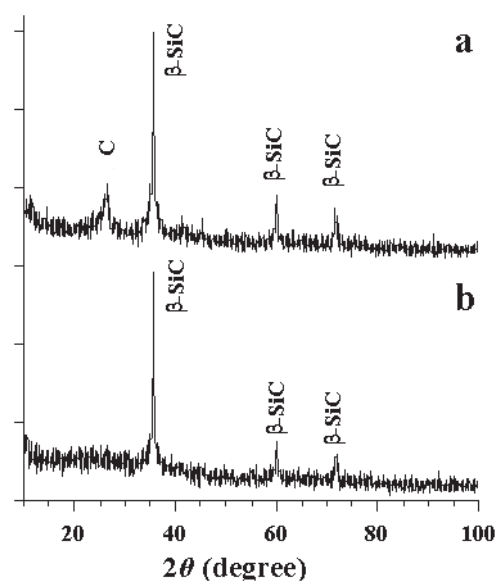

Figure 1. XRD patterns of the SiC nanotubes (a) as-synthesized and (b) after air treatment at 600°C for 2 h to remove the remaining unreacted carbon.

diffraction lines corresponding to SiC were observed. The SiC conversion could be tuned by adjusting the reaction conditions. Typical conversion of *ca*. 80 wt. % were obtained. This was explained by the carburization mechanism, *i.e.*, the well-known Shrinking Core Model, which states that the reacional interface is maximum at the beginning of the transformation and then regularly decreases as the reaction proceeds.[14,15] The formation, as a function of the transformation course, of SiC layers on the carbon surface, acting as a diffusion barrier for SiO and CO vapors, led to a progressive decrease in the rate of carburization.

The C to SiC transformation was accompanied by an increase in the specific surface area, from 20 m^2 g^{-1} up to ca. 40-50 m^2 g^{-1}. The SiC nanotubes synthesized had no microporosity. The increase in specific surface when going from carbon to SiC nanotubes was attributed to (*i*) the formation of a new porosity and (*ii*) the change in density during the transformation. The loss of one carbon atom as CO gas along with the density difference (between carbon and SiC) when going from C to SiC was probably responsible for the specific surface area increase, by formation of a new porosity, by the creation of voids and channels during the escape of CO molecules from the material. Similar results have already been reported during the study of SiC microtube synthesis starting from the low surface area and non-porous graphite filaments using the same synthesis method.[9] Volpe and Boudart have reported similar observations during the vapor phase carburization of solid MoO$_3$.[16] The oxide to carbide transformation was accompanied by an important increase in the specific surface area due to the change in the density and specific volume of the carbide when compared to its oxidic parent.

Figure 2 shows the SEM images of the starting carbon nanotubes and the corresponding SiC nanotubes. The general tubular morphology of the carbon precursor was completely retained after the carburization process, which highlighted the efficiency and the advantage of the SMS method in the conservation of the starting shape of the carbon material. It should be noted that the smooth surface of the MWNTs was transformed after carburisation into a more roughness one where holes and cracks can be visualized, in close agreement with the increase in surface area. No closure of the tube tip occurred during the synthesis, both inner and outer surfaces of the tubes also remaining accessible for further treatments. The SiC nanotubes had mean inner and outer diameters of *ca*. 30 and 100 nm respectively.

Oxidation of H$_2$S in a trickle-bed mode

Previous works showed that NiS$_2$ supported on SiC

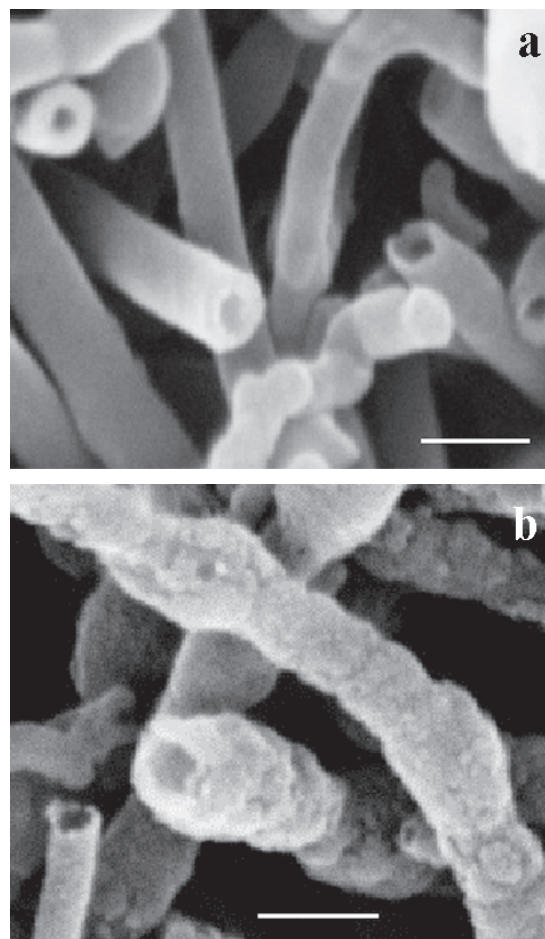**Figure 2.** SEM images of carbon (a) and SiC (b) nanotubes. The scale bars represent 100 nm.

grains displayed, for a velocity of 0.007 h^{-1}, a H$_2$S conversion of 100 % since the beginning of the test and for more than 100 h of time on stream.[3,6] Such a high performance for the selective H$_2$S oxidation was notably due to the mechanical removal of the sulfur formed from the active sites by a water film. The role of condensed water, acting as a conveyor belt on the catalyst surface when using SiC grains has already been reported and discussed in details.[3,13,17] A liquid water film allowed the sulfur formed to be removed from the NiS$_2$ active sites before the subsequent storage on hydrophobic SiC surfaces, outside the pores, which are free of active phase.

Performing the test at higher velocity (0.02 h^{-1}) in the present study, led to a completely different behavior of the catalyst in terms of activity (Figure 3). A few hour activation period was observed on the catalyst supported on SiC grains, attributed to the time required by the NiS$_2$ phase to be superficially transformed into a new active phase, an oxysulfide phase formed by the oxygen-sulfur exchange.[6,17] It should be noted that the catalyst rapidly deactivated as

a function of time on stream. This was attributed to the high space velocity and to the blockade of the active sites by the solid sulfur deposit. The transport phenomenon by water seemed to be insufficient at a high space velocity and thus, the solid sulfur formed remains on the active sites leading to deactivation by encapsulation.

Figure 3 shows the benefit use of SiC nanotubes as support for the NiS_2 phase. At a WHSV of 0.02 h^{-1}, the SiC nanotube supported catalyst still exhibited a H_2S conversion of 100 % since the beginning of the test and no deactivation was observed, even for more than 100 h of time on stream, for which the weight of accumulated solid sulfur on the material became greater than 200 wt. % of the starting weight of the catalyst. The absence of any visible activation period at the beginning of the test was attributed to a higher H_2S oxidation rate, which resulted from the tubular morphology of the catalyst. The sulfur selectivity remained at 100 % in good agreement with the low reaction temperature.[6,17,18]
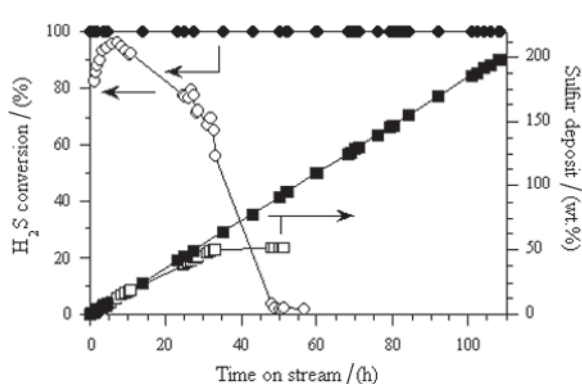

Figure 3. H_2S conversion and the corresponding solid sulfur deposit on the surface as a function of time on stream at 60 °C obtained for WHSV = 0.02 h^{-1} with the SiC nanotubes (filled symbols) and the SiC grains (empty symbols) as support. (H_2S = 2000 ppm vol., O_2 = 3200 ppm vol., H_2O = 20 % vol., balance He, O_2/H_2S = 1.6, catalyst weight = 3.35 g, WHSV = 0.02 h^{-1}).

It should be noted that most of the NiO phase, and also after the sulfidation step, its corresponding NiS_2 phase, was located inside the SiC nanotubes: TEM images only showed few NiO particles onto the outer walls of the tubes (not reported). The thickness of SiC rendered the material too much absorbent for electrons, and did also not allow the direct observation of nickel-based phases inside the tubes. EDS carried out on isolated SiC nanotubes proved however the presence of nickel inside the tubules (not reported). It was worth noting that the use of SiC nanotubes allowed to significantly improve both activity of the catalyst and the solid sulfur storage capacity for the low temperature oxidation of hydrogen sulfide. The impro-

vement in the storage capacity of the catalyst was attributed to the increase in the free volume of the nanotube material, which remained available for the sulfur storage during the reaction, when compared to the traditional grain size material. Taking into account that the void volume outside the tubes is much larger than outside the pores of usual mesoporous SiC grains, after the evacuation of solid sulfur outside the nanotubes by water, according to the same conveyor belt process, larger amounts of sulfur could also be stored in the external void volume, where only very few NiS_2 particles are located.

Figure 4 shows a SEM image of the active SiC nanotube supported NiS_2 catalyst after test and loaded with 200 wt. % of solid sulfur. Presence of solid sulfur outside the SiC tubes was clearly evidenced, although only very few particles of active phase was found on the outer walls of the catalyst as previously reported above. The sulfur having been formed where the reaction took place, *i.e.*, on the NiS_2 phase inside the nanotubes, one can assume that sulfur formed inside the SiC tubules was transported and then stored outside the tubular structure.
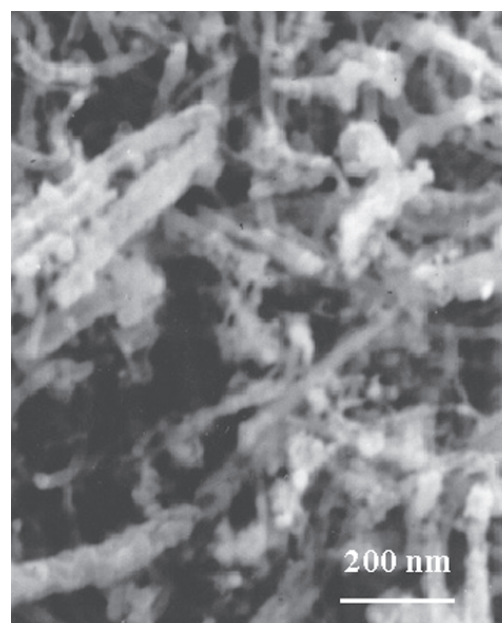

Figure 4. SEM image of the 200 wt. % sulfur loaded SiC nanotube-based catalyst after 100 h on stream at 60 °C.

The confinement effect

Baker and co-workers [19] proposed that the peculiar activity obtained for graphite nanofiber supported nickel catalysts for the hydrogenation of butadiene or crotonaldehyde was due to the specific morphology adopted by the nickel phase and induced by the strong interactions with the nanofiber support. Using a very

different kind of support, *i.e.*, SiC nanotubes, we had in the present study no evidence of the flat hexagonal morphology observed on graphite nanofibers by Baker and co-workers. In addition, the mean NiS_2 particle size inside the SiC nanotubes was estimated at about 20 nm by the XRD peak broadening method of Scherrer, similar to what was both observed by TEM and derived from the Scherrer technique on the NiS_2/SiC grains catalyst. No difference in the NiS_2 dispersion could be proposed. It appeared also interesting to develop a new idea, in order to explain the gain in activity when using the nanotube morphology as support : the inner partial pressure concept, or confinement effect due to the peculiar tubular morphology of the material.

The increase in WHSV led to a significant decrease in the H_2S conversion on the catalyst supported on SiC grains. Pieplu *et al.*[20] recently summarized in an extended review kinetic studies related to the direct and selective H_2S oxidation by O_2 to elemental sulfur. According to a traditional rate law with positive reaction order relative to H_2S, the increase in WHSV would be compensated by an increase in the H_2S partial pressure on the catalytic sites, in order to maintain the initial reaction rate, *i.e.*, H_2S conversion. It led to the development of a confinement concept in order to explain the observed results.

The inner partial pressure concept is based on the large increase of the H_2S partial pressure inside the SiC nanotubes, probably by microcapillarity phenomenon. In this concept, the apparent macroscopic H_2S partial pressure, outside the nanotubes, would remain unchanged, whereas the microscopic or nanoscopic partial pressure would significantly increase inside the nanostructure. Such a modification of the reactant partial pressure could probably occur during the flow through the tube, due to a tube wall effect and segregation phenomena between the different gaseous products. According to such a concept, one would expect that compounds with a high dipolar moment, *i.e.*, H_2S which is the less concentrated one among the reactants, would be the most affected during the diffusion through the tubule. A similar concept has been proposed by different authors such as Dillon *et al.*[21] and Liu *et al.*[22] for use of carbon nanotubes to improve hydrogen storage capacities. In the present study, the use of SiC instead of carbon and of H_2S as inlet reactant, a molecule presenting a permanent dipole, instead of more "inert" H_2 molecules in term of interactions with the surface, would both lead to more visible effects than in the works cited above. Concerning the nature of the used nanotubes, it is probable that the hydrophilic oxygen-containing surface layer was also formed during the synthesis of the SiC nanotubes. The carbon nanofiber to SiC nanotube transformation, along with the nanostructure

opening, could even favored such a partial oxidation of the inner SiC layer, due to the probable high defect density of the inner SiC nanotube surface. The highly hydrophilic nature of the nanotube inner surface would also increase the microcapillarity phenomenon.

Conclusions

Medium surface area β-SiC nanotubes prepared according to the Shape Memory Synthesis method was very successfully used as support material for the NiS_2-based active phase for the trickle-bed oxidation of H_2S into elemental sulfur at 60 °C. SiC nanotubes had mean inner and outer diameters of ca. 30 and 100 nm. The use of SiC nanotubes led to a significant increase in the overall catalytic performance, both in terms of activity and resistance to the solid sulfur deposition onto the material as compared to the reference catalyst supported on macroscopic SiC grains. The hypothesis of a confinement effect inside the SiC nanotubes has been advanced to explain the gain in activity observed. This confinement effect would lead to an increase in the partial pressure of H_2S inside the tubes compared to that outside the tubes which remained unchanged. The high capacity of solid sulfur storage on the material compared to that of macroscopic SiC grains has been explained by the large void volume outside the nanotubes when compared to the void volume outside of usual mesoporous and macroporous SiC grains.

Acknowledgements

References

1. Estep, J. W.; McBride Jr. G. T.; West, J. R.; *Advances in Petroleum Chemistry and Refining*, vol.6, Interscience: New York, 1962, ch 7.

2. Wieckowska, J.; *Catal. Today* **1995**, *24*, 405.

3. Keller, N.; Vieira, R.; Nhut, J. M.; N.; Pham-Huu, C.; Ledoux, M. J.; *J. Braz. Chem. Soc.* **2004**, in press.

4. Ledoux, M. J.; Nougayrède, J. B.; Savin-Poncet, S.; Pham-Huu, C.; Keller, N.; Crouzet, C.; *French pat. 97-16617*, **1997**.

5. Ledoux, M. J.; Pham-Huu, C.; Keller, N.; Savin-Poncet, S.; Nougayrède, J. B.; Bousquet, J.; *Catal. Today* **1999**, *53*, 535.

6. Keller, N.; Pham-Huu, C.; Estournès, C.; Ledoux, M. J., *Appl. Catal. A* **2002**, *234*, 193.

7. Keller, N.; Pham-Huu, C.; Ledoux, M. J.; *Appl. Catal. A* **2001**, *217*, 205.

8. Pham-Huu, C.; Keller, N.; Ledoux, M. J.; Charbonnière, L.J.; Ziessel, R.*; J. Mol. Catal. A* **2001**, *170*, 155.

9. Keller, N.; Pham-Huu, C.; Ledoux, M. J.; Estournès, C.; Ehret, G., *Appl. Catal. A* **1999**, *187*, 255.

10. Ledoux, M. J.; Guille, J. L.; Hantzer, S.; Dubots, D.; *US pat. 4 914 070*, **1990**.

11. Ledoux, M. J.; Pham-Huu, C.; Chianelli, R. R.; *Curr. Opin. Solid State Mater. Sci.* **1996**, *1*, 96.

12. Keller, N.; Pham-Huu, C.; Roy, S.; Ledoux, M. J.; Estournès, C.; Guille, J.; *J. Mater. Sci.* **1999**, *34*, 3189.

13. Ledoux, M. J.; Pham-Huu, C.; *CaTTech* **2001**, *5*, 226.

14. Hurst, N. W.; Gentry, S. J.; Jones, A.; McNicol, B. D.; *Catal. Rev.-Sci. Eng*. **1982**, *24*, 233.

15. Falconer, J. L.; Schwartz K. A.; *Catal. Rev.-Sci. Eng*. **1983**, *25*, 141.

16. Volpe, L; Boudard, M.; *J. Solid State Chem.* **1985**, *33*, 332.

17. Ledoux, M. J., Pham-Huu, C.; Keller, N.; Nougayrède, J. B.; Savin-Poncet, S.; Bousquet, J.; *Catal. Today* **2000**, *61*,157.

18. Klein, J.; Henning, H. D.; *Fuel* **1984**, *63*,1064.

19. Chambers, A.; Nemes, T.; Rodriguez, N. M.; Baker, R. T. K; *J. Phys. Chem. B* **1998**, *102*, 2251.

20. Pieplu, A.; Saur, O.; Lavalley, J. C.; *Catal. Rev. Sci. Eng.* **1998**, *40*, 409.

21. Dillon, A. C.; Jones, K. M.; Bekkedahl, T. A.; Klang, C. H.; Bethune, D. S.; Heben, M. J.; *Nature* **1997**, *386*, 377.

22. Liu, C.; Fan, Y. Y.; Liu, M.; Cong, M. T.; Cheng, H. M.; Dresselhaus, M. S.; *Science* **1999**, *286*, 1127.